Surfactant foams doped with laponite: unusual behaviors induced by aging and confinement

R. M. Guillermic, A. Salonen, J. Emile and A. Saint-Jalmes

Received 22nd July 2009, Accepted 15th September 2009
First published as an Advance Article on the web 12th October 2009
DOI: 10.1039/b914923f

We report results on foams stabilized by surfactant (sodium dodecyl sulfate) and containing clay particles (laponite). We have studied how these foams age with time (drainage and coarsening) and their rheological properties. Due to the doping with laponite, which provides an additional time evolution of the foaming fluid itself, unusual behaviors are observed: especially, drainage arrest and re-start and enhanced elasticity are observed as a function of time. These results can be interpreted in terms of both confinement of the laponite inside the foam liquid channels, and competition between the laponite aging and the one of the foam (controlled by its own physical parameters). By playing with these foam parameters and those of the bulk solution containing laponite, we can control the time evolution and these non-monotonous features. Qualitatively, it is found that time, laponite concentration and confinement have all the same effect, enhancing the jamming of the interstitial fluid inside the foam.

1 Introduction

The dispersion of a gas inside a fluid—an aqueous foam—behaves very differently from its two main components. The dispersion is actually neither a gas, nor a liquid, but shares the properties of both, and even those of an elastic solid.[1–4] Such specific behaviors are the origins of the wide use of foams by engineers in industry, as foams often turn out to be the best compromise in many practical situations.[1,3]

It is indeed striking to note that an aqueous foam is actually a state of matter which is very difficult to define, as it can have a large range of possible behaviors. An aqueous foam can be opaque or transparent, conductive or not, soft or rigid, *etc*… One of the reasons for the complexity of foams is that they are hierarchically organized at different lengths: the scale of the gas-fluid interface where surfactants are adsorbed (nm), the scale of the thin films separating the bubble faces (tens of nm), the scale of the interconnected fluid channels, called "plateau borders" (from tens of microns to mm), the scale of the bubble itself (from a hundred microns to cm), and finally the macroscopic scale of the sample (cm to m). As a consequence of this organization, the macroscopic features are complex and they results from subtle balances between effects occurring at these various lengthscales, having all their own amplitude and timescales. Another consequence is that the foam properties depend both, and in very intricate ways, on its physical properties (bubble diameter D, liquid fraction ε = volume of liquid/volume of foam, dimension and shape of the sample), and on its chemical components. Furthermore, the foam properties are not static: starting from a freshly made wet foam, one just has to wait to pass through very different behaviors. This is due to the irreversible aging which causes the liquid fraction ε to decrease (drainage),[5–7] and the bubble diameter D to grow (coarsening).[8–10] In that respect, simply with time, as a result of the irreversible decrease of ε and increase D, any foam becomes drier, more transparent, more resistive, more elastic, its volume changes, *etc*…; and all these variations are significantly large. These are reasons which makes aqueous foams rather unique materials.

Recently, there has been more and more understanding of these issues: one understands better the links between the different lengthscales, how foam ages, and the balance between what depends on the physical parameters and the chemical ones in all the foam features.[6,4,7,11] In that respect, today, considering the fact that the basic phenomenon ruling the foam properties are—at least partly—better understood, it becomes relevant to try to go beyond the classical low molecular weight surfactant foams with their irreversible aging behaviors, in order to develop new regimes and materials useful for new applications. This approach can be followed either by creating new physical conditions (liquid fraction, bubble size, polydispersity, *etc*…), or by using new chemical components. Along the chemical path, foams can actually be stabilized by compounds other than the usual low molecular weight surfactant or soap molecules; as for emulsions, proteins or solid particles can replace the surfactants.[12–15] Also, within the liquid bulk, one can add additives to modify the bulk properties; for instance, there has been already some experiments with elastic and non-newtonian fluids.[16] Here we have investigated another class of foaming fluid: a surfactant solution is doped with clay particles (laponite) so that this fluid develops its own aging behavior, meaning that its viscoelastic properties change with time. In this work we show how the intrinsic dynamics of the foaming fluid can be coupled with that of the foam, in order to obtain new foam properties and aging behaviors.

2 Chemicals and experimental methods

2.1 Solutions and gas: preparation and characterization

We start with a foaming solution, containing a classical anionic surfactant, sodium dodecyl sulfate (SDS) and pure water

Institut de Physique de Rennes, CNRS UMR 6251, Rennes 35042 Cedex, France

(Millipore). The concentration is fixed at $c_{SDS} = 4$ g L^{-1}, above the critical micellar concentration. This provides a good foamability of the SDS solution itself, and prevents film ruptures and foam collapse. This SDS solution is then doped with laponite RD. It is a synthetic clay obtained from Laporte, Ltd. Each particle is a colloidal disk with a diameter of 30 nm and a height of about 1 nm. In this work, we have added laponite up to a concentration $c_L = 20$ g L^{-1}. Once the laponite is added to the SDS solution, the solution is stirred at 1000 rpm for 10 min; then, it is either studied in bulk, or poured into the foam production apparatus. We use a MCR301 rheometer (Anton Paar) for studying the rheology of the solutions: oscillatory and steady-shear measurements are performed with a plate–plate geometry, with various gaps.[17]

The dispersed gas is always an important component for a foam, as its properties control the foam coarsening.[10,7] To obtain different rates of increase of D, we use two gases: nitrogen (N_2) and perfluoroethan (C_2F_6). The differences are both in the solubility and diffusivity. With C_2F_6 the coarsening rate is reduced by typically 30 times when compared to N_2.[10,7]

2.2 Foam production and characterization

The foams are produced by a turbulent mixer method.[18] It consists of a T-junction through which strong gas stream and liquid jets are mixed, and it is similar to a milli-fluidic device operating at high pressure. The initial mean bubble diameter is $D_0 = 100$ μm, and independent of ε and of the chemical components. This device allows us to tune the foam liquid fraction ε from 0.02 to 0.4, while the polydispersity in size remains low.[18] The device provides a fast rate (5 L/min), with good spacial homogeneity and uniformity of the liquid fraction at time zero. The advantage of this high production rate is twofold. First, it gives a well defined time origin for the foam age. Secondly, as the solution is highly sheared in the constriction of the T-junction, one can consider that the laponite solution is strongly rejuvenated at this time, thus also setting a controlled time origin for the fluid age.

We use this T-junction device to fill a plexiglass cylindrical cell (height = 30 cm, diameter = 5 cm). Once the foam is injected, at an initial liquid fraction ε_0, we monitor the decrease of the liquid fraction $\varepsilon(t)$ by measuring the electrical conductivity along the vertical direction: 10 pairs of electrodes, separated by 2 cm, are incrusted along the cell height. From these measurements we deduce the absolute liquid fraction thanks to a calibration valid in the whole range of ε.[19]

For the rheological studies on foams, we have developed a home-made cone–plate geometry (diameter = 17 cm, angle = 10°) suited for the MCR301 rheometer. The foams are injected directly from the production device from the center of the bottom plate, in between the cone and the plate. Typical oscillatory measurements (amplitude and frequency sweeps[17,4,20]) are then performed as a function of age.

We also studied the structure and stability of single thin films, using the film balance apparatus.[21,22] This technique provides information at the intermediate scale of the thin film, corresponding to two gas-liquid interfaces facing each other at short distances (<100 nm). By video-microscopy, we can observe the texture and features of the film, and measure the thickness at various applied pressures (corresponding to various liquid fractions once transposed inside a foam). Such measurements also show how the interfaces interact, and by which mechanisms they repel each other allowing the films to be stabilized. We have also performed surface tension and interfacial dilational rheology measurements with the pendant drop technique. Note that this technique cannot be fully used, especially in terms of interfacial rheology because the aging and jamming of the solution (as described below) prevent valid measurements of the interfacial contributions.

3 Experimental results

3.1 Bulk results

The rheological bulk measurements confirm that the SDS/laponite solutions are systems undergoing a strong aging. Fig. 1 shows the results of oscillatory measurements (frequency $f = 1\ s^{-1}$, and amplitude $\gamma = 0.01$) as a function of time: complex viscosity μ^* in Fig. 1a, and elastic and viscous moduli G' and G'' in Fig. 1b. For all the concentrations, the viscosity increases drastically with time; as well, it is found that the higher the concentration, the higher the viscosity (at a given time). Fig. 1b helps to understand the equilibrium between elastic and viscous contribution in the complex viscosity. With time, the elastic modulus finally dominates, and the solutions always become more elastic than viscous. As can be seen in Fig. 1b, the time for G' to become higher than G'' is shorter when increasing c_L. We also report results of steady-shear viscosity at a fixed shear rate (1 s^{-1}) (Fig. 2). Typically, within an hour, the viscosity

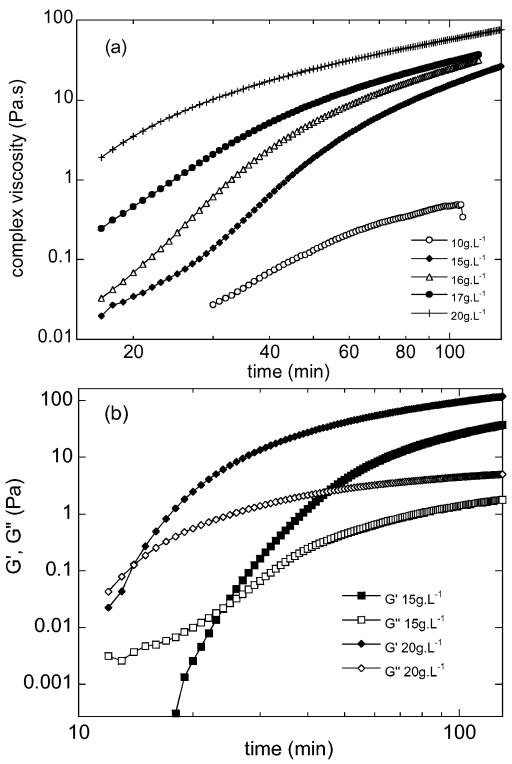

Fig. 1 Oscillatory rheometry on the bulk solutions: (a) complex viscosity *vs* time for various laponite concentrations c_L; (b) G' and G'' *vs* time for two laponite concentrations.

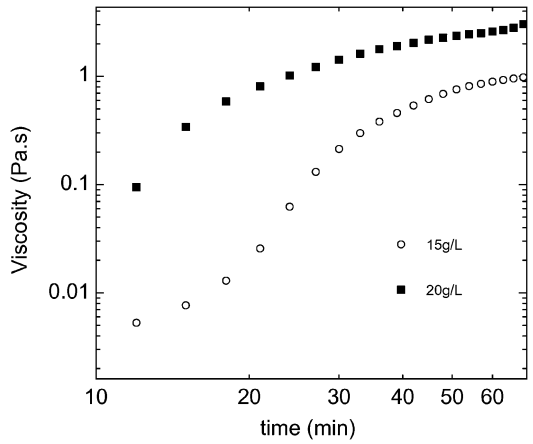

Fig. 2 Viscosity at constant shear rate as a function of time, for two laponite concentrations. The viscosity varies by about 2 orders of magnitude in an hour.

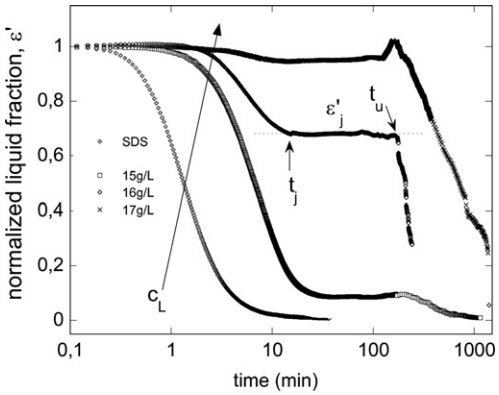

Fig. 3 Time evolution of the normalized liquid fraction ε' at a fixed position inside the foam, for SDS foams and various concentration of laponite c_L. On the curve at $c_L = 16$g/L, the times t_j and t_u, and the normalized liquid fraction ε'_j are indicated.

increases by almost 3 orders of magnitude. Qualitatively, note that aging and laponite concentration have the same effect. Thus, these SDS-laponite solutions act like complex fluids, with controlled non-Newtonian properties. Finally, one must point out that we have recovered here results consistent with previous rheological works on bulk laponite and on its aging.[23–27] The origin of this viscosity increase and jamming of the fluid is still under debate, and can either be interpreted as a glass transition, a gelification due to clusters of increasing size, or like a "castle of cards" networks. The difficulty arises from the fact that there are probably different microscopic structures (depending on the amount of laponite, or added salt) and that all provide the same macroscopic aging features. In the conditions used here, with a large concentration of added surfactants, one can expect to be within the gel-like phases of the phase diagram.

3.2 Foam stability results

First, the addition of laponite does not reduce the perfect foaming of the SDS solution. The produced laponite-doped foams look very similar to the SDS ones: there are no exotic structures, the sample does not look like a gel with separated bubbles, but one can see compressed bubbles and a network of plateau borders circulating between them, as for usual foams.

Experiments with the thin film balance device show that—with laponite—the films are thin and homogeneous; indeed, they appear very similar to those made only of SDS with equilibrium thickness between 10 to 50 nm,[21,22] depending on the applied pressure. The foam structural stability is thus mostly controlled by the SDS adsorbed at the interfaces, and the laponite particles do not drastically modify the film thickness and texture. As well, the surface tensions of the solutions with laponite are found to be very close to the ones of the pure SDS solutions (measured by the pendant drop technique). All together, the results at intermediate scales agree with the visual observations that the laponite-doped foams looks identical to the SDS ones, in terms of microscopic structures or foam organization (interfaces, films attached to plateau borders, all connected by nodes[5]).

Once the foams are made and injected in the cylindrical cell, they are free to age by drainage and coarsening. Fig. 3 illustrates how foams made with N_2, and with $D_0 = 100$ μm drain for different laponite concentrations: the normalized liquid fraction, $\varepsilon' = \varepsilon/\varepsilon_0$ (where ε_0 is the value obtained at time zero, just after foam production), at a given position z is plotted *vs* time. For laponite concentrations lower and up to 10 g L^{-1}, one sees no effect of the laponite on the foam drainage, and the foam behaves as the ones made of only SDS. For an intermediate range of concentrations, typically 16 g L^{-1} in Fig. 3, drainage fully stops at a given time (defined as t_j) and at given liquid fraction (defined as ε'_j), and eventually drainage restarts (at a time t_u). As can be seen in Fig. 3, for $t_j < t < t_u$, the liquid fraction is really constant, and this is the first time that a clear plateau is observed experimentally in such drainage curves. Lastly, for the highest concentrations (above 18 g L^{-1}): we observe no drainage for time t as long as a few hundreds of min. However, even at these high concentrations, the foams always eventually drain at long times. The results of Fig. 3 are for $\varepsilon_0 = 0.15$ and N_2; varying this initial liquid fraction from 0.08 to 0.2 does not change the results described above: qualitatively, the same arrest and re-start of drainage are observed whatever the initial liquid fraction.

In complement, Fig. 4 shows the behavior along the vertical axis z for the concentration $c_L = 16$ g L^{-1}. The same arrest and re-start occur everywhere in the sample. However, the arrest and restart of drainage are not found at a unique ε'_j, and not at the same times t_j and t_u. As z increases (going down inside the sample; $z = 0$ at the top of the foam), ε'_j, t_j and t_u increase. Another way of describing the drainage results of Fig. 4 is for a long time range (here between 50 and 200 min), there are no variations of the liquid fraction through the whole sample, and the foam remains "frozen" with a vertical constant gradient of liquid fraction. This is clearly different from a foam without laponite, which is fully drained in less than 30 min.

Three other experimental observations must be reported. First, these features also depend strongly on the gas used. Fig. 5 shows that, qualitatively, the same results are found with C_2F_6, but ε'_j, t_j and t_u are bigger. Secondly, associated to the re-start of drainage at t_u, we observe, for intermediate vertical positions z, a small increase of ε' just before its drastic fall, as it can already be seen in Fig. 3, 4 and 5 (this is more marked at high c_L, when ε'_j is high). For

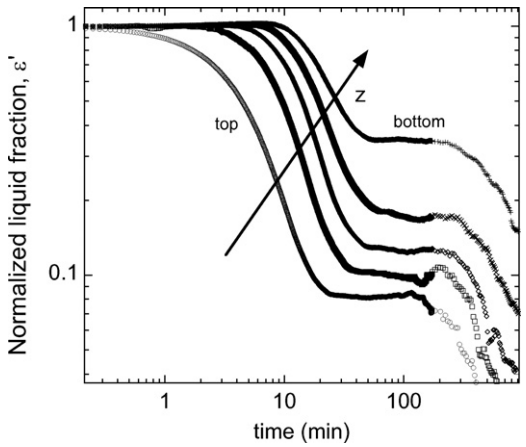

Fig. 4 Time evolution of the normalized liquid fraction ε' at a fixed laponite concentration ($c_L = 16$g/L), for different vertical positions z.

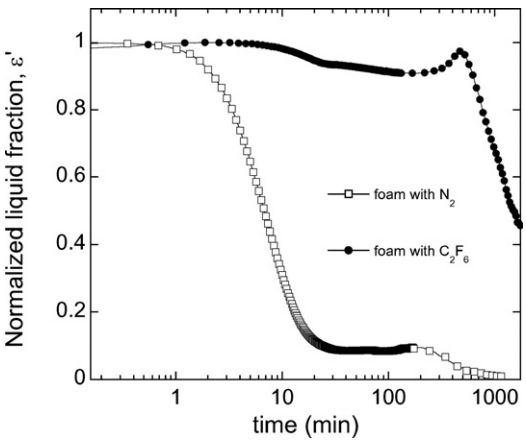

Fig. 5 Time evolution of the normalized liquid fraction ε' at a fixed position inside the foam for the two gases used ($c_L = 16$g/L).

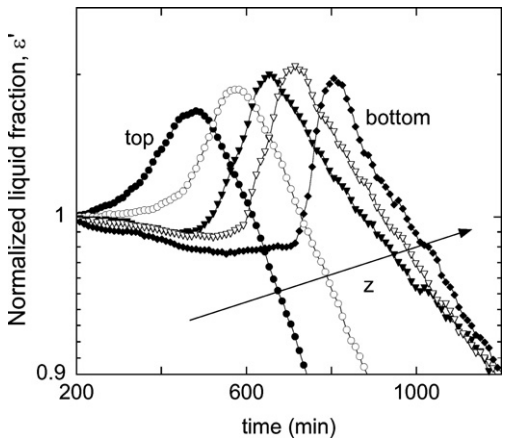

Fig. 6 Normalized liquid fraction ε' *vs* time for different vertical positions z: zoom on the bump observed at all z, and travelling downward (indicated by the arrow). The laponite concentration is $c_L = 18$ g L^{-1}.

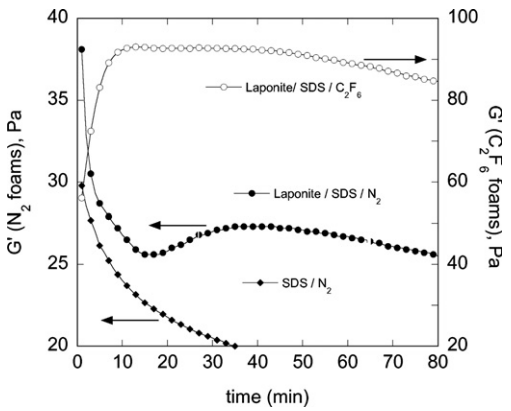

Fig. 7 Elastic shear modulus *vs* time for foams of different chemical compositions.

a given sample, focusing on this bump, it is found that it propagates downward inside the foam: Fig. 6 shows how the bump and the strong decrease occur at each electrode position z, one after the other, with increasing time t_u. In Fig. 6, this effect is illustrated with a foam containing $c_L = 18$ g L^{-1} of laponite.

Thus, we have found very unusual results for the way the foam loses its interstitial fluid, and experiments show that this is strongly linked to the amount of laponite, and to the gas. Note that previous works on dispersed systems (emulsions, or foams) containing laponite focused on the foamability (with low concentrations of laponite) and almost not at all on the aging of the materials produced.[28,29]

3.3 Foam rheology results

We have studied the rheological response to small amplitude oscillations: as for the bulk measurements, the frequency is fixed at 1 Hz and the amplitude is 0.01. Fig. 7 presents the time evolution of the storage modulus G' as a function of the chemical composition: SDS/laponite/N_2, SDS/laponite/C_2F_6, and SDS/N_2, for a fixed laponite concentration $c_L = 15$ g L^{-1}. Depending on the chemicals, G' behaves differently: it irreversibly decreases for SDS/N_2, it strongly increases first and then slightly decreases at long times for SDS/laponite/C_2F_6, and even a complex time-dependent behavior is observed in the case of SDS/laponite/N_2. Note that the range of G' are not the same for the three chemical systems, and that high values are reached with laponite and C_2F_6 (3 times bigger than the maximum value found at t = 0 for the other systems). As well, the case of SDS/C_2F_6 is not shown here, but remains mostly flat, as already observed.[30] Concerning, the loss modulus G'', similar qualitative features are observed.

In the striking non-monotonous situation of SDS/laponite/N_2, the effect of the laponite concentration is shown in Fig. 8. As the concentration increases, the time at which the modulus starts to grow decreases; inversely, the amplitude of the growth increases with c_L. At the highest concentration, the initial value of G' is well above those found at lower c_L, but only a single decrease of G' is subsequently observed. Thus, as for their time evolution shown in Fig. 3–5, the SDS foams doped with laponite show very unusual mechanical properties.

4 Discussion

In the following section, we analyze the data, in order to find the origins and mechanisms responsible of the non-classical properties described before.

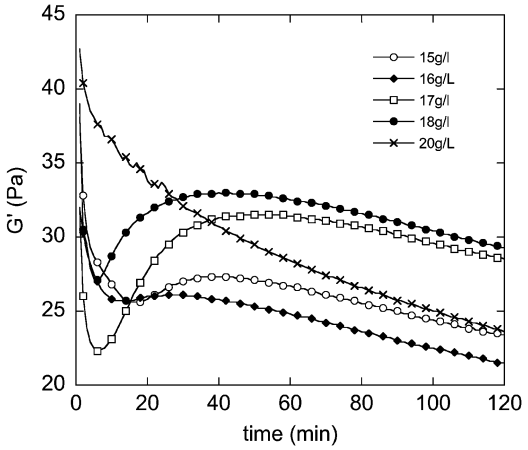

Fig. 8 Evolution of G' *vs* time for different concentrations of laponite in the SDS/Laponite/N_2 foams.

First, we briefly recall what is happening in a classical surfactant foam, corresponding to the case of a SDS foam without laponite. Drainage and coarsening have their own timescales. The typical drainage time for the free-drainage situation (corresponding to a foam of height H, with uniform initial liquid fraction ε_0, and bubble diameter D) can be written:

$$t_d = \frac{H\mu}{K\rho g D^2 \varepsilon_0^{\alpha}} \quad (1)$$

where μ is the fluid bulk viscosity, ρ the fluid density, g the gravitational acceleration, K a dimensionless permeability constant, and α is between 0.5 and 1.[5–7] The value of this exponent and of K depend on the interfacial mobility; this mobility describes the coupling between the flow within the plateau borders and the flow within their interfaces. For this coupling, the relevant microscopic interfacial properties turns out to be the shear viscosity of the gas–liquid interfaces.[6,7]

We also describe the typical behavior for $\varepsilon(z, t)$ during free-drainage. For a given z (not close to the top or the bottom, where edge effects occur) the liquid fraction remains constant during a time t_r: this corresponds to the retardation time required for the drainage (starting at the top) to reach this location. Then, the liquid fraction ε decreases, following a power law, $\varepsilon \propto t^{-\beta}$, with an exponent $1 < \beta < 2$, also depending on the interfacial mobility.[5–7] An important point for the discussion is to emphasize that t_r, the time for the beginning of drainage increases with z: it arrives later and later as going down into the sample.

At the microscopic scale, the drainage can be seen as a flow of liquid through the network of interconnected plateau borders, in response to gravity and capillarity. So, the typical radius of curvature r of the plateau border triangular-like cross-section gives the scale of the pore within the foams.[5–7] The fluid network structure can be modelized in order to relate the liquid fraction ε to this radius r and to the plateau border length L:

$$\varepsilon = 0.17(r/L)^2 \quad (2)$$

As well, the length L is related to the bubble diameter D such as: $D = 2.7L$ for a model Kelvin-type bubble.[6] Theoretically, Eq. 2 is valid only for dry foams ($\varepsilon < 0.1$), but experiments tend to show that it remains valid almost up to 0.15–0.2. In this case, the triangular-like cross section of a plateau border is Cr^2, with $C = 0.4$. The above theoretical description illustrates one of the major specificities of foam drainage (when compared to flow in solid porous media): the pore size depends on the liquid fraction and bubble size; in particular, during a free-drainage experiment, the pore size irreversibly decreases with time. The second important difference with flow in porous media is that one must take into account the interfacial mobility, as discussed previously (Eq. 1).[6,7]

The typical coarsening time of a foam is:

$$t_c = \frac{D^2}{D_{eff} h(\varepsilon) f(\varepsilon)} \quad (3)$$

The effective diffusion coefficient D_{eff} includes the gas properties (solubility, diffusivity and molar volume), the surface tension Γ, and the thickness of the films separating the bubbles h; its dependance on the liquid fraction is not trivial and is enclosed in the non-dimensional function $h(\varepsilon)$.[10,7] The coarsening time includes a second dimensionless function $f(\varepsilon)$, describing the area of the bubble covered by thin films (through which gas diffusion occurs), normalized by the total bubble area. This relative area covered by films, and $f(\varepsilon)$ as well, strongly decreases when increasing ε:[10] quantitatively, this function f represents the major contribution of the liquid fraction in t_c.

It is known that there can be some coupling between drainage and coarsening: when coarsening occurs during drainage, the two effects are enhanced and are strongly accelerated.[7,10] During drainage, if the bubbles are getting bigger, this will lead to faster drainage (Eq. 1), implying a drier foam and then even faster coarsening (Eq. 3), *etc*… With $D_0 = 100$ μm, a SDS/N_2 foam is precisely in the situation of simultaneous drainage and coarsening; while for SDS/C_2F_6, the drainage occurs without coarsening.[7] So, significantly slower drainage and coarsening are usually found for C_2F_6 foams, when compared to N_2 foams.[7]

With this type of classical aging behavior in mind, it is first obvious that the observed arrest of drainage seen in Fig. 3–5 does not fit with the previously observed results and models. Such an arrest implies that the flow within the plateau borders is fully stopped. It is also rather straightforward to see that the simple increase of the fluid shear viscosity is not a sufficient argument to explain the jamming of the fluid. First, because viscosity can only reduce the fluid velocity (Eq. 1) and secondly because the bulk values of μ, at the typical times of arrest in the foam, are still less than a few hundred times the viscosity of water.

This full arrest requires that the fluid effective viscosity becomes infinite, and that the fluid gets jammed. In other words, the gravitational force must become too small to provide flow and the gravity-induced stress σ_g is smaller than a yield stress σ_y. In order to verify if our results can be interpreted in such a framework, we first need to estimate the typical stresses encountered inside the foams. From the liquid fraction and the bubble diameter (Eq. 2), we get that the pore characteristic dimension r is of the order 10 to 50 microns. Similarly, from the measured fluid drainage velocity v, which is between 0.05 mm/s to 1 mm/s for these foams,[31] we can estimate the shear rate $\dot{\gamma}$ inside the plateau borders, and thus the shear stress $\sigma_g = \mu\dot{\gamma}$ responsible of this velocity. We can only give the range of stresses, as μ, r and v are not constant with time, and change with the experimental conditions (laponite concentration, gas, *etc*…). Nevertheless, we

end up with typical stresses inside the foam of the order of 1–10 Pa. The fact that the solution is restricted to narrow plateau borders provides a situation where the fluid flows extremely slowly, corresponding to low stresses. Moreover, with time, the fluid confinement increases due to shrinking of the plateau borders section: this reduces the speed ($v \propto r^2$ (Eq. 1–2)) and thus the gravitational stress acting on the fluid.

For comparison, we need to measure independently the yield stress of the solution. As the confinement acts on the fluid velocity, we must also wonder about the role of the confinement on the yielding. As shown in Fig. 1b, the elastic modulus eventually dominates the viscous one with time; this means that the oscillations performed for these measurements are below the yielding of the fluid. For determining the yield strain and stress, we have thus done amplitude-sweep experiments, where the amplitude is increased at constant frequency. This is done at two values of the gap between the rheometer plates, to investigate the role of confinement. Fig. 9 shows the results of G' and G'' *vs* time ($c_L = 15$g/L). For a large gap, the elastic part is well below the viscous one (no yielding). However, at the lower gap, an elastic contribution dominates at $\gamma < 1$. Moreover, a clear signature of yielding is observed: G'' finally dominates G' and the yield strain γ_y can be localized at the kink in G' (arrow in Fig. 9). Then we can experimentally determine the yield strain, from which we deduce the yield stress $\sigma_y = G'\gamma_y$, as a function of time for the two confinements, and two concentrations (Fig. 10). The yield stress strongly increases with time, concentration but also with the confinement. Such an effect of confinement was already discussed and seen in other systems.[32,33] Note that the confinement effects are already detectable at gaps which are still large when compared to the size of a single laponite molecule, meaning that the fluid is most likely organized with supra-molecular arrangements of laponite/SDS complexes; the size of such structures increases with time, inducing all the aging effects seen in bulk (Fig. 1, 2 and 10).

Now, when comparing the ranges of gravitational and yield stresses, it turns out that—thanks to the confinement and the restriction of the flow inside plateau borders of small sections—it becomes possible that σ_y reaches a few Pa inside the foam (Fig. 10), easily enough to overcome σ_g. In that respect, the effect of the confinement is to reduce strongly the fluid velocity and the gravitational stress σ_g. In parallel, the confinement in the plateau

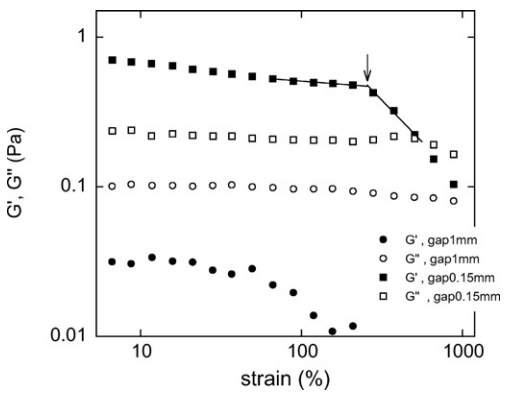

Fig. 9 Bulk amplitude sweep results: viscoelastic moduli *vs* strain, for two values of the gap. The arrow indicates the yield point.

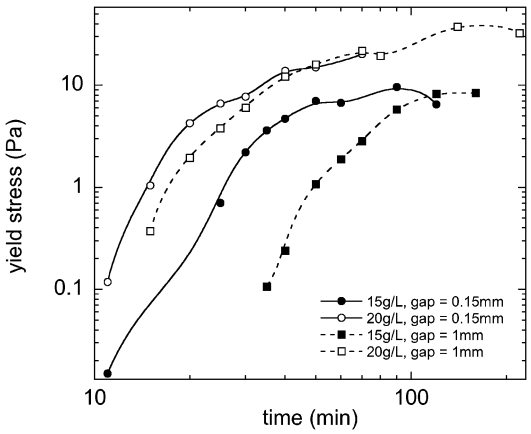

Fig. 10 Yield stress as a function of time, for two values of the gap and two concentrations. Lines are guides for the eyes.

borders helps the solution to becomes more elastic than viscous, it increases the yield stress σ_y, in order to allow the fluid to get jammed (once $\sigma_y > \sigma_g$).

The combination of this confinement (which is modified by the foam aging) with the aging of the laponite, can finally explain the other features of Fig. 3 to 5. The fact that ε'_j and t_j depend on z is a direct consequence of the dynamics of the laponite. As stated before, as z increases, the foam starts to drain later (the plateau border shrinking and velocity reduction come later); since it arrives at longer times, the fluid jamming requires a lower degree of shrinking because the yield stress has, in parallel, increased with time. Thus, ε'_j has to be bigger.

So, these foams are indeed more complex than those made out of a simple yielding fluid having a constant yield stress value; the observed features can only be seen because of the effect of the confinement and aging on the laponite. It is interesting to point out that laponite concentration, time and confinement act the same way: as the concentration, time or confinement are increased, the solution becomes more and more viscoelastic, and it develops an increasing yield stress. This explains why the curves of Fig. 3, Fig. 4 and Fig. 5 are qualitatively identical: the same fluid jamming effect is found, but through different means.

This interpretation is also validated by preliminary experiments at $D'_0 = 1$ mm. For such larger initial bubbles, and for the same range of c_L added, nothing is observed in drainage. In agreement, with the results described before, there is never enough confinement in these foams: the plateau border cross section is typically 10 times bigger (Eq. 2) and the drainage time is thus divided by 100 (Eq. 1) when compared to experiments at D_0; as a consequence, the drainage is fast and the experiments do not last long enough for the laponite to develop a yield stress and to get jammed.

However, the data of Fig. 3 and 4 show that the fluid jamming is not permanent, and in all the cases the foam always finally drains. We interpret this drainage re-start and unjamming of the fluid at t_u as a consequence of the foam coarsening with time. In fact, even if drainage has stopped, gas diffusion and coarsening continue; the observation of single thin films show that the films are always thin and that they do not block the gas. Following Eq. 2, this means that, at fixed ε, an increase of D implies an increase of r. With time, the size of the channels increases, the

confinement is lost and the gravitational stress becomes bigger than the yield stress. This is more proof that, without enough constriction, the foam simply drains and the interstitial fluid flows. This coarsening effect is fully validated by the data seen in Fig. 5 for the two gases. With C_2F_6, one gets a slower coarsening and consequently the re-start occurs later. Note also that the slow coarsening has also reduced the drainage speed because of the coupling between the two effects;[10,7] it is then normal that ε'_j is higher for C_2F_6.

We can then also understand the origin of the bump associated with the re-start (Fig. 6). The drainage re-start must begin at the foam top: the foam is always dryer there (Fig. 4), as a result of the previous initial drainage (before the jamming), so it coarsens faster at the top (Eq. 3). As the fluid unjamming occurs at the top, some liquid is freed and starts to flow: it expand the plateau borders (as in the experimental situation called "forced-drainage"[5]), and this further help to remove the jamming. A pulse of fluid is thus initiated at the top, and it finally travels downward.

The analysis of the rheological results is also based on the balance between foam aging and laponite aging. First, as for drainage, it is clear that a simple increase in viscosity is not sufficient to provide the increase of G'. Previous works showed that an increase in viscosity by 3 orders of magnitude has almost no effect on G'.[30] In fact, the elastic modulus can usually be written:

$$G' \propto (\gamma/D)g(\varepsilon) \quad (4)$$

where $g(\varepsilon)$ is a decreasing function of only ε.[4,20] Therefore, at fixed ε, $G' \propto 1/D$. The results found for SDS/N_2 foams are in agreement with Eq. 4: G' continuously decreases as the foam coarsens. Similarly, with C_2F_6 and no laponite, D and ε remain constant (over the rheological measurement time), implying that G' does not change.

Thus, when compared to the cases without laponite, the increase of G' seen with C_2F_6 and laponite can then only be due to the gradual jamming of the fluid inside the Plateau borders with time; however, it is not trivial to quantitatively understand these variation of G': the mechanical situation is indeed complex as it corresponds to a time-dependent yield fluid (laponite solution) confined inside another yield fluid (foam). In any case, at long times, coarsening finally dominates over laponite aging and G' slowly starts to decrease. For the case of SDS/Laponite/N_2 at $c_L = 15$ g L^{-1}, the curve is more complex than with C_2F_6 because coarsening is faster and actually play a role at short times. The data can be understood by considering that coarsening occurs first (as the bubbles are initially small, Eq. 3, leading to the decrease of G', Eq. 4) then the fluid jamming within the foam occurs and dominates (G' increases), and lastly, coarsening finally relaxes the confinement and the fluid jamming (G' decreases). This competition between effects increasing or decreasing G' is well illustrated in Fig. 10; for instance, an earlier and stronger fluid jamming is found when the laponite concentration is increased.

5 Conclusions and outlook

We have shown that doping SDS foams with laponite is responsible for new and non-classical aging and mechanical properties, without changing the foam structure. Interestingly, we have shown that it is possible to block the fluid at a given time and given value; and that it can be re-delivered after some waiting time. We have been able to interpret these behaviors as the results of a balance between the aging of the foam (drainage and coarsening), the one of the laponite and the confinement in the plateau borders. We have found that the fluid gets jammed because the confinement decreases the gravitational stress while it raises the yield stress. Similarly, it is important to point out that time, laponite concentration and confinement act the same way and provide the same jamming of the interstitial fluid. In that respect, it seems feasible to adjust these blocking and delivery features by playing with the foam bubble size, liquid fraction, mixture of gas, concentration of laponite, *etc*…

Such non classical behavior could be used for optimizing filtration processes, or for designing materials with control delivery; the original and time-dependent mechanical properties might also be of interest for cosmetics or for construction materials (cement, paints…). Another point of interest is that the foams at high concentrations of laponite do not drain (at least for much longer period of time than usual): this provides samples suitable for studies at constant liquid fraction, which is something usually impossible to do on the ground because of the gravitational drainage. As a first example and thanks to the doping with laponite, we are now investigating the acoustic properties of coarsening foams at constant liquid fraction, as a function of time, bubble size, and physical-chemistry.

Acknowledgements

The authors thank the Agence Nationale pour la Recherche (ANR-07-blan-0340) for financial support.

References

1 R. K. Prud'homme and S. Khan, *Foams: Theory, Measurements, and Applications*, Marcel Dekker Inc., New York, 1997.
2 D. Weaire and S. Hutzler, *The Physics of Foams*, Oxford University Press, New York, 1999.
3 A. Saint-Jalmes, D. Durian, and D. Weitz, *Kirk-Othmer Encyclopedia of Chemical Technology*, 5th edn, (John Wiley and Sons, New York, 2004, vol. 8, p. 697.
4 R. Hoehler and S. Cohen-Addad, *J. Phys.: Condens. Matter*, 2005, **17**, R1041.
5 S. A. Koehler, S. Hilgenfeldt and H. A. Stone, *Langmuir*, 2000, **16**, 6327.
6 H. A. Stone, S. A. Koehler, S. Hilgenfeldt and M. Durand, *J. Phys.: Condens. Matter*, 2003, **15**, S283.
7 A. Saint-Jalmes, *Soft Matter*, 2006, **2**, 836.
8 D. J. Durian, D. Weitz and D. Pine, *Phys. Rev. A: At., Mol., Opt. Phys.*, 1991, **44**, R7902.
9 S. Jurine, S. Cox and F. Graner, *Colloids Surf., A*, 2005, **263**, 18.
10 S. Hilgenfeldt, S. A. Koehler and H. A. Stone, *Phys. Rev. Lett.*, 2001, **86**, 4704.
11 S. Tcholakova, N. D. Denkov, K. Golemanov, K. P. Ananthapadmanabhan and A. Lips, *Phys. Rev. E*, 2008, **78**, 011405.
12 B. Binks, *Curr. Opin. Colloid Interface Sci.*, 2002, **7**, 21.
13 V. Schmitt, C. Cattelet and F. Leal-Calderon, *Langmuir*, 2004, **20**, 46.
14 A. Cervantes Martinez, E. Rio, G. Delon, A. Saint-Jalmes, D. Langevin and B. P. Binks, *Soft Matter*, 2008, **4**, 1531.
15 S. Tcholakova, N. Denkov and A. Lips, *Phys. Chem. Chem. Phys.*, 2008, **10**, 1608.
16 M. Safouane, A. Saint-Jalmes, V. Bergeron and D. Langevin, *Eur. Phys. J. E*, 2006, **19**, 195.

17 H. Barnes, J. Hutton, and K. Walters, *An Introduction to Rheology*, Elsevier, Amsterdam, 1989.
18 A. Saint-Jalmes, M. Vera and D. J. Durian, *Eur. Phys. J. B*, 1999, **12**, 67.
19 K. Feitosa, S. Marze, A. Saint-Jalmes and D. J. Durian, *J. Phys.: Condens. Matter*, 2005, **17**, 6301.
20 S. Marze, R. Guillermic and A. Saint-Jalmes, *Soft Matter*, 2009, **5**, 1937.
21 V. Bergeron, *J. Phys.: Condens. Matter*, 1999, **11**, R215.
22 C. Stubenrauch and R. von Klitzing, *J. Phys.: Condens. Matter*, 2003, **15**, R1197.
23 H. Cummins, *J. Non-Cryst. Solids*, 2007, **353**, 3891.
24 D. Bonn, H. Kellay, H. Tanaka, G. Wedgam and J. Meunier, *Langmuir*, 1999, **15**, 7534.
25 A. Knaebel, M. Bellour, J. P. Munch, V. Viasnoff, F. Lequeux and J. L. Harden, *Europhys. Lett.*, 2000, **52**, 73.
26 P. Levitz, E. Lecolier, A. Mourchid, A. Delville and S. Lyonnard, *Europhys. Lett.*, 2000, **49**, 672.
27 D. Bonn, H. Tanaka, G. Wegdam, H. Kellay and J. Meunier, *Europhys.Lett.*, 1999, **45**, 52.
28 S. Zhang, Q. Lan, Q. Liu, J. Xu and D. Sun, *Colloids Surf., A*, 2008, **317**, 406.
29 N. Ashby and B. Binks, *Phys. Chem. Chem. Phys.*, 2000, **2**, 5640.
30 S. Marze, A. Saint-Jalmes and D. Langevin, *Colloids Surf., A*, 2005, **263**, 121.
31 A. Saint-Jalmes, Y. Zhang and D. Langevin, *Eur. Phys. J. E*, 2004, **15**, 53.
32 G. Meeten, *Rheol. Acta*, 2000, **39**, 399.
33 C. Nugent, K. Edmond, H. Patel and E. Weeks, *Phys. Rev. Lett.*, 2007, **99**, 025702.

